# PROPELLER ANALYSIS USING A HYBRID NAVIER-STOKES/FREE-WAKE METHOD

Byung-Young Min, Brian E. Wake, Patrick O. Bowles, Claude G. Matalanis, Blake Moffitt
United Technologies Research Center, East Hartford, CT, USA

E-mail: minb@utrc.utc.com

**Abstract**

A hybrid Navier-Stokes/Free-wake method has been introduced for an efficient and accurate propeller analysis. A solution sensitivity study has been performed to find a proper propeller modelling approach. This includes time-step size, number of sub-iterations, and number of free-wake trailers. The method has been validated against three experimental propellers, which have measured data in terms of integrated thrust, power and efficiency. Also, cross comparison with full Navier-Stokes simulations and conventional propeller blade element method has been conducted. The results showed very good correlation with measured data and at least as good correlation as full Navier-Stokes simulations. The blade element method, which relies on CFD generated airfoil tables, showed good correlation in relation to thrust and power but tended to have the poorest correlation of propeller blade angle. Also, it was found that a small scale experimental propeller may experience large region of laminar flow due to its low Reynolds number. Overall, the introduced hybrid method showed accurate propeller simulation capability capturing geometric effects by first principals with at least one order of less computational time compared to full Navier-Stokes simulation, yet holding capability of yawed inflow simulation.

## NOMENCALTURE

$C_c$ : Section chord-wise force coefficient

$C_n$ : Section normal force coefficient

$C_P$ : Power coefficient $\left(=\frac{P}{\rho n^3 D^5}\right)$

$C_q$ : Section torque coefficient

$C_T$ : Thrust coefficient $\left(=\frac{T}{\rho n^2 D^4}\right)$

$C_t$ : Section thrust coefficient

$D$ : Diameter

$J$ : Advance ratio $\left(=\frac{V_\infty}{nD}\right)$

$n$ : Rotation per Second (RPS)

$P$ : Power

$R$ : Radius

$T$ : Thrust

$V_\infty$ : Freestream velocity

$\beta$ : Blade pitch angle

$\eta$ : Propeller efficiency $\left(=\frac{JC_T}{C_P}\right)$

$\rho$ : Density

$\tilde{\nu}$ : Normalized S-A working variable

$ref$ : Reference value

## 1. INTRODUCTION

Recently, growing interest in high speed rotorcraft led to compound helicopter configurations being considered as candidates for next generation helicopters. Recent examples that are already flying include Sikorsky's X2 Technology™ Demonstrator, and Airbus' X3. These high-speed rotorcraft configurations, although quite different, both use propellers as high-speed thrust generators. As the propeller contributions to vehicle performance become more important for high-speed flight performance, accurate propeller performance prediction becomes more important for optimal vehicle design. Historically, blade-element-methods (BEM) were mainly used for propeller performance prediction. The BEM provides reasonably good prediction with a very fast simulation time. However, the methods do not capture some known three-dimensional effects and are limited to regions where the minimum energy loss wake assumption is appropriate. Recent Reynolds-Averaged Navier-Stokes (RANS) simulations provide good predictions based on first principals [1] but come with significant increase in computational cost. Additionally, pitch

variations of CFD model often require a new mesh generation step, especially if the propeller model is attached to a center-hub, which increases the time to solution. In this study, a hybrid Navier-Stokes/Free-wake method is introduced for an efficient high fidelity propeller analysis. The hybrid method has proven to be an efficient method with a prediction capability comparable to full RANS simulations for rotors in forward flight [2,3], rotors in hover [4], and wind-turbines [5]. Propeller simulations is another good application area of the hybrid method as the wake convection is often well defined, and it can be used for yawed inflow as well with less mesh requirements.

The objective of the current study is to establish a proper hybrid method modelling approach for propeller simulation and to validate the proposed method against three experiment wind-tunnel test data in terms of propeller performance. Also, cross check with conventional full CFD and BEM approaches are made to assess its level of accuracy.

## 2. ANALYSIS METHODOLOGIES

### 2.1. UT-GENCAS and Hybrid Method

UT-GENCAS, a hybrid Navier-Stokes/Free-wake method solver [4], is used in the current study. It is a generic compressible Navier-Stokes solver with Lagrangian free-wake model for wake modeling. Roe's finite-difference scheme (FDS) with 3rd order MUSCL was used for inviscid flux computation, and 2nd order central-difference scheme was used for viscous flux computation with thin-layer assumption. A two-equation Kinetic Eddy Simulation (KES) model [6] and a one-equation Spalart-Allmaras model are availabel for turbulence closure. After solution insensitivity was found to turbulence model, the Spalart-Allmaras model was used in this study. A 2nd-order implicit time-marching scheme was used with a multi-grid method for faster sub-iteration convergence.

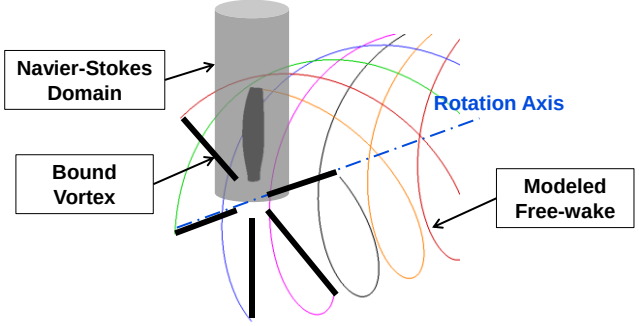


Figure 1. Illustration of hybrid method for propeller simulation

Figure 1 illustrates the hybrid method. In this hybrid method, only a single blade is modeled with the Navier-Stokes equations. All other blades and wakes are modeled with a bound vortex and free-wake filament trailers. The wake effect can be modeled with single strong tip-vortex, or distributed multi-trailers can be included in addition to tip-vortex wake. The wake strength is determined by the sectional propeller loading, and the impact of wake and bound vortices are applied to the Navier-Stokes domain through the induced velocity boundary condition at outer domain boundaries. The mesh requirement is about 1/n less than full Navier-Stokes simulation, where n is the number of propeller blades. This indicates that the mesh size does not increase with number of blades. Since the Navier-Stokes solver is used for the flow field surrounding the blade, the geometric effects are directly captured based on first principals.

In the current study, default setting was 10 trailers with the most outer trailer representing tip vortex. All the trailers were maintained up to 5 revolutions. Wake filaments were shed every 5 degrees, and the N-S simulation proceeded 0.25 degree per time step. Solution sensitivity to some of the parameters are included in the later section.

### 2.2. Full Navier-Stokes Solver

#### 2.2.1. UTCFD

UTCFD is a Reynolds-averaged Navier-Stokes code (RANS) using the Lax-Wendroff multiple grid scheme of Ni [7]. It is an internal UTC turbomachinery numerical method developed and continuously used for decades. It is capable of handling structured and unstructured grids, but a structured grid was used for this propeller simulation. It uses a two-equation $\kappa-\omega$ turbulence model.

#### 2.2.2. STAR-CCM+®

STAR-CCM+® is a commercial CFD software package developed and distributed by CD-adapco [8]. It is employing a unstructured mesh with local grid refinement ability. Its surface wrapping capability enables easy and fast turn-arond time from raw CAD to CFD simulation. From the range of solution options, a coupled implicit solver was used with *k-ω* turbulence model in steady state single passage simulation mode.

### 2.3. Blade Element Method (BEM)

The BEM code used in this study is a in-house code described and validated in Reference [9]. The code

can use either the Prandtl approximate solution or the Goldstein exact solution to the circulation function relating to a minimum energy loss wake. For the propeller geometry and operating conditions used in this paper, results using the Goldstein circulation function were nearly identical to the Prandtl model. The code contain modifications from traditional BEM codes to handle highly loaded blades, large propeller hubs, propeller sweep, and non-uniform inflow velocities. The propeller model was built by discretizing the blade into multiple spanwise stations (10 for Propeller-A, 20 for Propeller-B, and 13 for Propeller-C). Airfoil drag polars at the spanwise stations were calculated using 2D CFD.

### 2.4. Propeller Models and Computational Grids

#### 2.4.1. Propeller-A

The first propeller is a 4-bladed model scale propeller with swept tip. The propeller was tested in United Technologies Research Center (UTRC) Main Wind-Tunnel. The test rig has a long cylindrical center-body extended in the upwind direction to reduce propeller hub effects. The model propeller radius is 19.5 inch with maximum chord approximately 3.7 inch. From the test, data from range of blade pitch angles and advance ratios are available. The corresponding Reynolds number at 0.75R ranges from 1.2 M to 1.6 M.

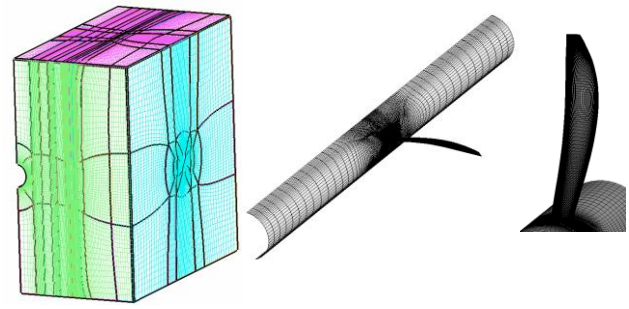

Figure 2. Grid system for hybrid UT-GENCAS

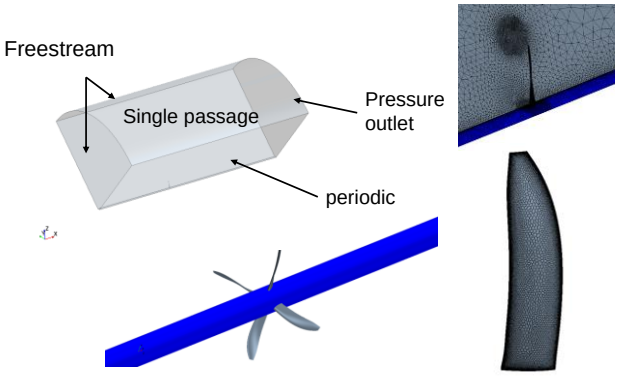


Figure 3. Grid system for STAR-CCM+

Figures 2 and 3 show grid systems for UT-GENCAS (hybrid method simulation) and STAR-CCM+ (steady single passage simulation), respectively. The hybrid method grid has rectangular domain surrounding single blade. The center-body is included as viscous wall. It has 192 x 128 (chord-wise x span-wise) grid cells on the blade surface with average wall y+ value less than 1. Total cell count is 3.25 M cells for single blade. The outer domain of the grid is at least 10 chords away from the blade. For blade pitch modification, grids only around blade are deformed. The STAR-CCM+ model is an unstructured grid with refinement around tip to resolver tip-vortex. It has prism layer around blade to resolve viscous layer, but the center-body was modelled as slip-wall. The total cell count for single blade passage is 10.7 M. For fast run-time, steady state simulation was carried out for this STAR-CCM+ approach. It is noted that the blade has slightly different swept from the hybrid method grid because of error in blade build-up from airfoils. The error was found later, but it is believed that its impact to performance measure is not significant. For BEM simulation, airfoil tables were generated using STAR-CCM+ for the thick inboard sections blending into the propeller hub and MSES [10,11] for the remaining sections.

#### 2.4.2. Propeller-B

The second propeller is a 6-bladed small scale representative aviation propeller with standard propeller airfoil sections. The model was tested in the small-scale Pilot Wind-Tunnel (PWT) of United Technologies Research Center (UTRC). Figure 4 shows the installed propeller at the PWT, and Table 1 summarizes the test condition. Integrated thrust, power and efficiency data are available for code validation.

Table 1. Propeller B test condition

| | Propeller Test Model |
|---|---|
| Radius | 8 inch |
| Blade Count | 6 |
| Adv. Ratio, $J$ | 1.6 |
| RPM | 4200 |
| Freestream Velocity | 150 ft/s |
| $M_{tip}$ | 0.26 |
| $M_{inf}$ | 0.13 |
| $Re_{0.75R}$ | 0.18 M |

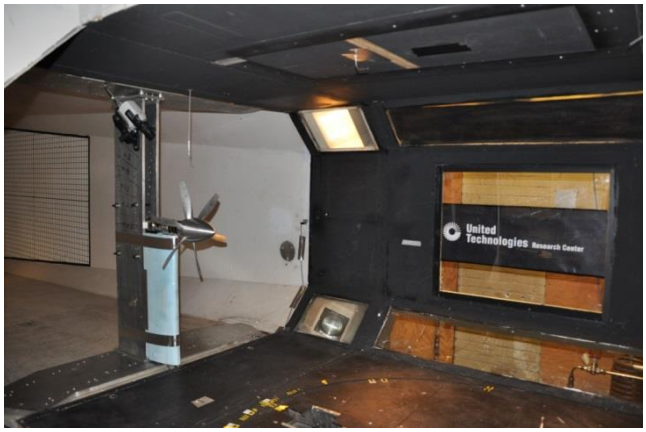


Figure 4. Propeller-B in UTRC pilot wind-tunnel

Figure 5 shows the grid system for UT-GENCAS. For this simulation, the center-body was not included. The grid count for single blade is 4 M cells with 256 x 120 (chord-wise x span-wise) cells on the blade surface. The average wall y+ value was about 0.1. A full Navier-Stokes simulation using UTCFD for this propeller has been published in reference [1] by current authors. In order to compare it with current hybrid method, the result is reproduced from reference [1]. Figure 6 is a reproduced grid figure from reference [1]. This model includes center-body and tunnel wall. Total grid count was 38.5 M cells with 256 x 108 (chord-wise x span-wise) cells on the blade surface. Its average wall y+ value was about 0.2. The full-wheel rotation was achieved with sliding interfaces in the front, back and top of the propeller. A new grid was generated for each blade pitch angle. For BEM simulation, airfoil tables were generated using CFL3D 2D simulation.

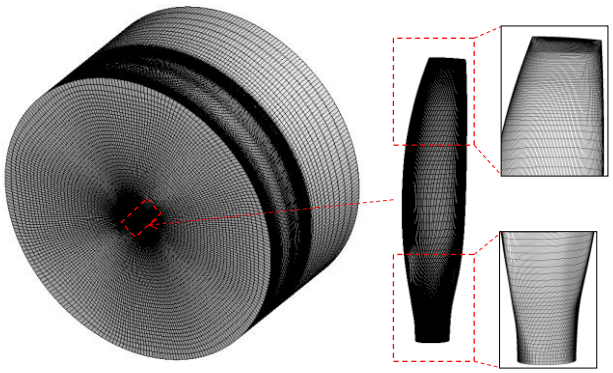

Figure 5. UT-GENCAS grid for propeller-B

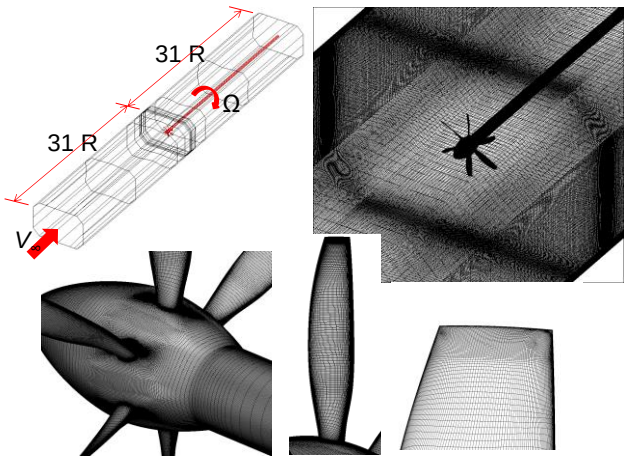


Figure 6. Full Navier-Stokes UTCFD grid for propeller-B, reproduced from refernce [1]

### 2.4.3. Propeller-C

The propeller-C was also tested in UTRC's PWT with the same rig as used for propeller-B. This propeller test and validation provides an additional data set to assess robustness of the analysis solver. The grid topology and cell count of the propeller-C for UT-GENCAS is very similiar to propeller-B shown in Figure 5.

## 3. RESULTS

### 3.1. Solution Sensitivity Study

The initial setting for UT-GENCAS, a hybrid method, was to use 10 trailers with the last trailer representing rolled-up strong tip-vortex. The wake filaments were shed every 5 degrees and they were maintained for 5 revolutions. This wake model was based on previous experience in helicopter analysis. For a helicopter in forward flight, a single strong tip-vortex filament is often sufficient as it is responsible for most of downwash in forward flight. However, a propeller blade is highly twisted with relatively low aspect ratio. Thus, the span-wise blade loading distribution may vary rapidly. This leads to rapid bound vortex strength variation, and the inboard trailing vortices may not be negligible, which requires multiple trailers. The inboard trailers are uniformly distributed, and the strength represents delta-bound vortex strength between neighbouring blade span. Figure 7 shows an example of wake filaments and Figure 8 shows example time history of solution convergence. The free-wake geometry is dominated by freestream velocity rather than self-induced velocity, and this makes the hybrid method more stable for propeller simulation. From the time history plot, it shows that the simulation converged in less than 2 revolutions even at high pitch cases.

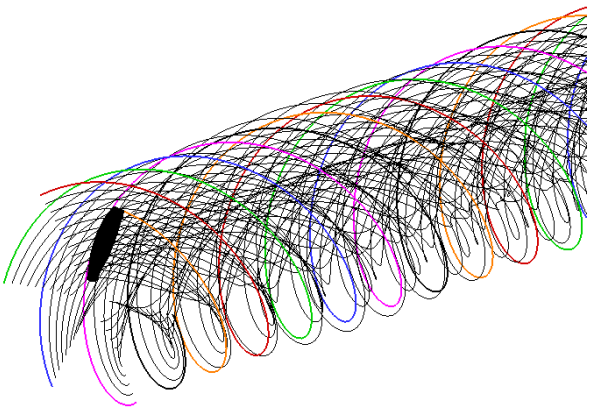

Figure 7. Example of free-wake geometry

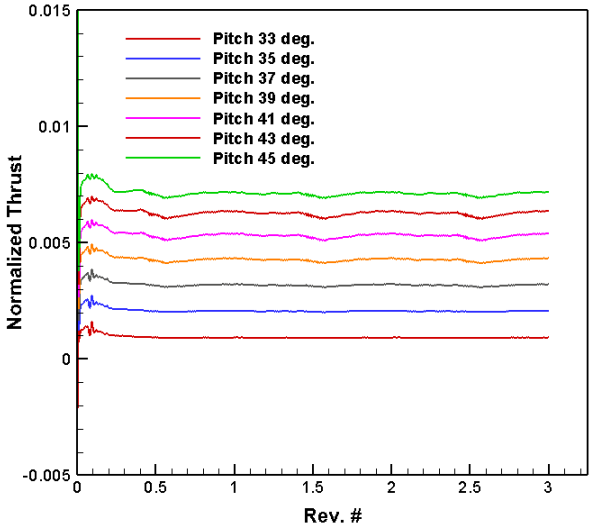


Figure 8. Example time history of solution convergence

In order to assess solution sensitivity to number of trailers and to obtain converged solution, the number of trailers was varied from a single trailer to 10 and 20 trailers, while maintaining 0.25 degree per time step with 30 sub-iterations. The study was performed using Propeller-B at a high pitch condition. Figure 9 compares thrust and efficiency for each case. Results from 10 and 20 trailers are identical, whereas the single trailer model shows 14% more thrust and 1% higher efficiency. Figure 10 compares the normal force distribution from each case. The 10 and 20 trailer models are almost identical, but the single trailer predicted higher normal force throughout the blade, indicating a lack of induced velocity compared to multi-trailer models. A sub-iteration convergence study was also carried out with same propeller at both low and high pitch conditions, while maintaining time step of 0.25 degree per step and 10 trailers. Figure 11 compares resultant thrust and efficiency. The values were normalized with 30 sub-iteration results at both pitch conditions. The 15 sub-iteration shows 7% lower thrust and 4% lower efficiency compared to 30 sub-iteration case, but the 50 sub-iteration case did not show much difference from the 30 sub-iteration case at both pitch conditions. For the time step convergence study, simulations for propeller-A were performed using blade advancement of 0.1, 0.25 and 1 degree per time step with 30 sub-iterations and 10 trailers. For a constant high pitch angle, advance ratio sweep was conducted. Figure 12 compares normalized efficiency and Figure 13 compares normalized thrust. The results show that 1 degree per time step is too coarse, but 0.25 degree per step is as good as 0.1 degree per step. Therefore, time step of 0.25 degree and 30 sub-iterations with 10 trailers were used for the rest of study. Additional solution sensitivity study for grid independence has not been performed since 3-4 M cells per blade seems sufficient from past experience in helicopter simulation, which typically involves more complex flow phenomena.

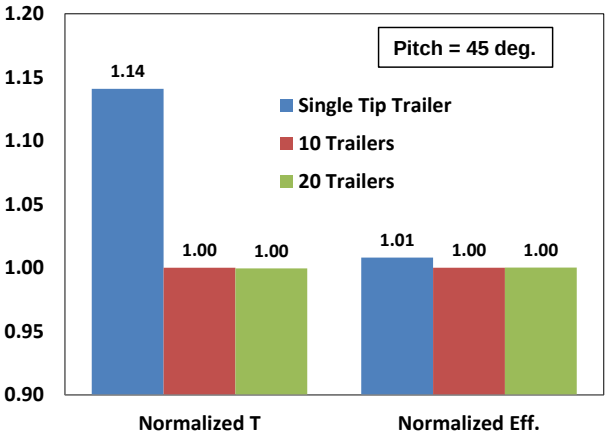


Figure 9. Solution sensitivity to number of trailers

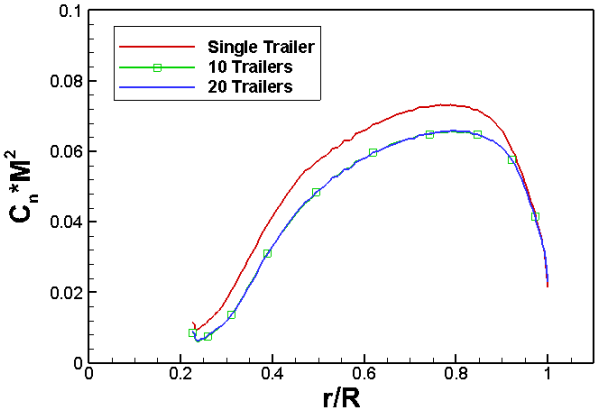


Figure 10. Normal force distribution, Pitch=45 deg.

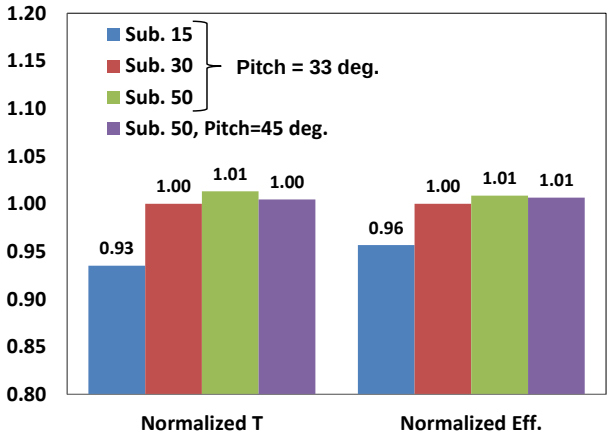


Figure 11. Sub-iteration convergence

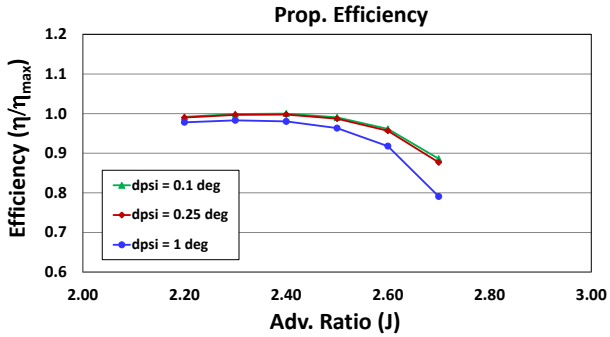


Figure 12. Time step convergence: efficiency

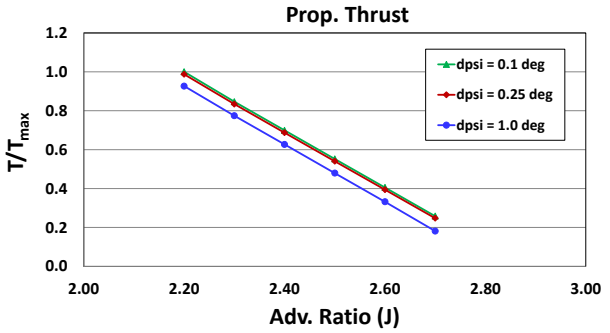


Figure 13. Time step convergence: thrust

### 3.2. Propeller-A

The propeller-A has swept blade planform shape consisting of 4 blades at large scale. In the experiment, blade pitch was set constant with fixed tunnel speed, and the propeller RPM was varied to change advance ratio. A correlation study has been performed for pitch angles from 38 degree to 46 degree with a range of advance ratios. The hybrid method results are compared to measured data as well as STAR-CCM+ and BEM simulation results. Figure 14 compares normalized efficiency and Figure 15 compares normalized thrust as a function of advance ratio. First, both UT-GENCAS and STAR-CCM+ show similar correlation with measured data with slight under-prediction of efficiency before the efficiency stalls. At high advance ratios, STAR-CCM+ shows more delayed stall although data points are coarse. In thrust prediction, UT-GENCAS shows consistently better correlation with measured data in most cases, but both simulations over-predicted thrust. Since efficiency is consistently under-predicted, this indicates a torque over-prediction. A potential contributor to the error could be turbulent transition. The Reynolds number is less than the critical Reynolds number until quarter-chord at 0.75R, and a large portion of the blade may experience laminar flow. Both simulations, however, were performed using an assumption that the flow was fully turbulent. Figure 16 and Figure 17 compare efficiency as function of thrust at constant advance ratio of 2.0 and 2.2, respectively. Slight under-prediction is noticed, but overall good correlation is observed from both CFD simulations. Also included are predictions from BEM simulation. At these two conditions, the BEM shows best correlation with measured data. However, Figure 18, shows that as for set propeller blade angles, the BEM results tended to be shifted as compared to the UT-GENCAS and experimental results. Thus, the BEM results correlate well with the relationship between thrust and power, but have a poorer correlation with the propeller blade angles required to provide a given thrust at a set advance ratio.

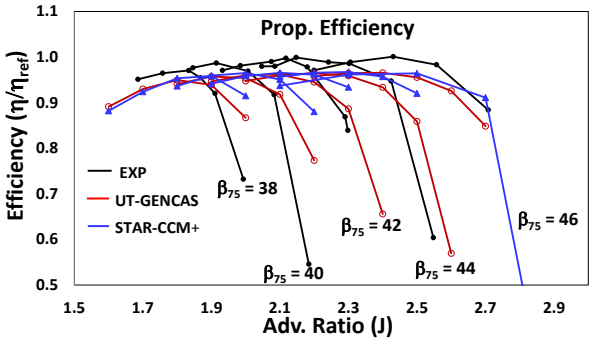


Figure 14. Efficiency comparison: Propeller-A

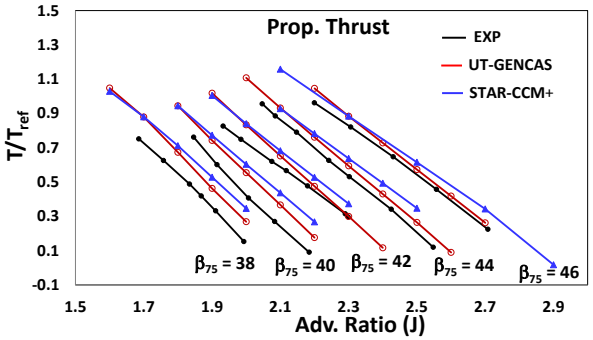


Figure 15. Thrust comparison: Propeller-A

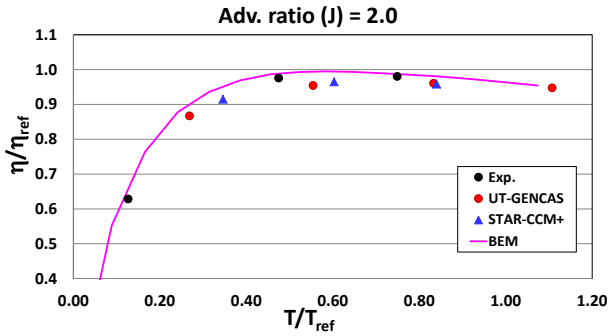


Figure 16. Efficiency at J=2.0: Propeller-A

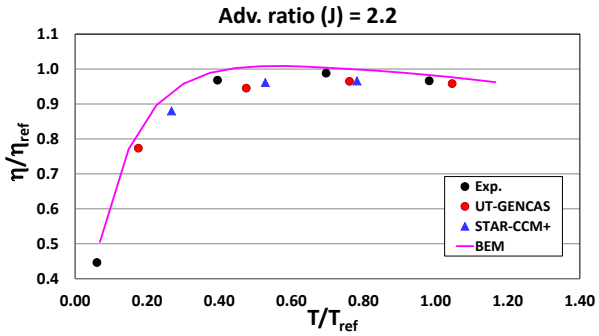


Figure 17. Efficiency at J=2.2: Propeller-A

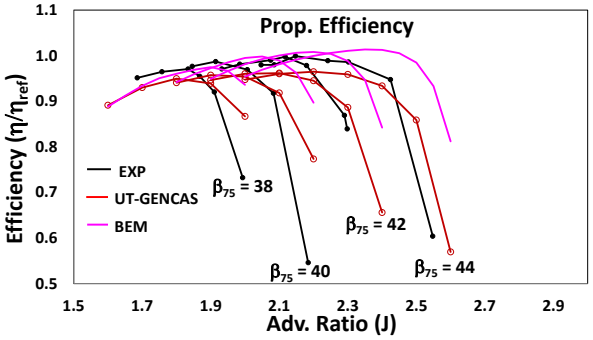


Figure 18. Efficiency comparison with BEM: Propeller-A

### 3.3. Propeller-B

The 6-bladed small scale propeller-B was validated at a constant advance ratio of 1.6 at the tunnel wind Mach number of 0.13. Its RPM was fixed and blade pitch angle was varied so that the thrust coefficient ranges from 0.05 to 0.3, approximately. Figure 19 and Figure 20 compare predicted power and efficiency to the measured data. It includes results from both UT-GENCAS and BEM. The predictions from both simulations are close, but show slight under-prediction of power. The difference is more amplified in the efficiency curve, showing over-prediction from both simulations. It is noted that the UT-GENCAS simulation was carried out using fully turbulent assumption with Spalart-Allmaras turbulence model. The BEM used CFD generated 2D airfoil tables, and the tables were also generated using RANS with fully turbulent Spalart-Allmaras model. The Reynolds number at 0.75R of this small scale blade is about 0.18 M, which is much less than critical Reynolds number of flat plate (~0.5 M). Thus, fully turbulent assumption may not be proper for this scale of propeller. In order to examine this further, the freestream value of the S-A model working variable, $\tilde{\nu}$, was varied at a high pitch condition. This may not guarantee physically accurate turbulent characteristics prediction such as wind-tunnel turbulence intensity, length scale, or transition on the blade, but it may provide solution sensitivity and clue for the error. The efficiency variation according to $\tilde{\nu}$ is plotted in Figure 21. It was found that the efficiency jump occurs at a certain level of $\tilde{\nu}$ value. After examining the flow field, it was found that eddy viscosity production was nearly negligible before the efficiency jump occurs, and the flow was maintained as practically laminar. The efficiency at this state agreed with measured data. With same low $\tilde{\nu}$ value for freestream, UT-GENCAS simulation was repeated for other pitch angles and the correlation is plotted in Figure 22 and Figure 23. These show very good correlation in both power and efficiency with low freestream $\tilde{\nu}$ value. Although not included here, it was confirmed that a laminar simulation with the turbulence model turned-off shows the same results. Figure 24 compares surface flow pattern from both laminar and fully turbulent cases at a pitch angle of 39 degree. The propeller has thick inboard airfoils and sharp leading edge at outboard section. This leads to trailing edge separation at inboard and leading edge separation at outboard. With fully turbulent flow, the separation is supressed at both inboard and outboard area, producing higher thrust. Figure 25 compares blade loading distribution from the two cases at same pitch angle. Higher section normal force and thrust is observed from full turbulence case. The section torque is also higher with fully turbulent flow, but the increase in thrust

leads to higher efficiency, as the efficiency is defined as $\eta = JC_T/C_P$ and $J$=1.6 in the current condition. Also included in Figure 22 and Figure 23 is a result from a full-wheel simulation using UTCFD, published in reference [1]. The UTCFD simulation used the κ–ω turbulence model with a long inlet computational domain. Close examination of the solution showed that the inlet turbulence decayed quickly, and flow around blade has a very low level of turbulence eddy viscosity. This resulted in better correlation than the fully turbulent UT-GENCAS simulation. However, UT-GENCAS with a practically laminar flow simulation showed best correlation throughout the range of thrust.

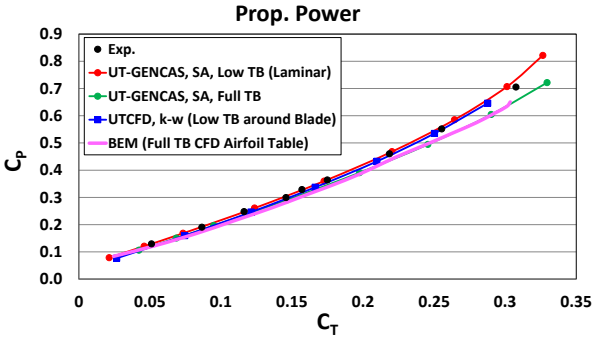


Figure 22. Power with low freestream $\tilde{\nu}$

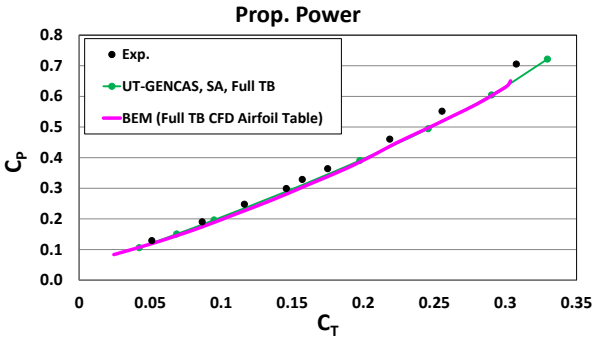


Figure 19. Propeller-B power vs. Thrust

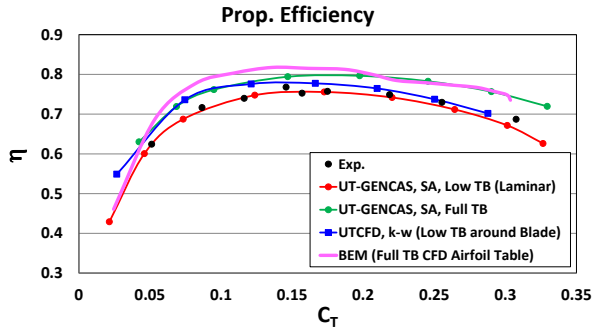


Figure 23. Efficiency with low freestream $\tilde{\nu}$

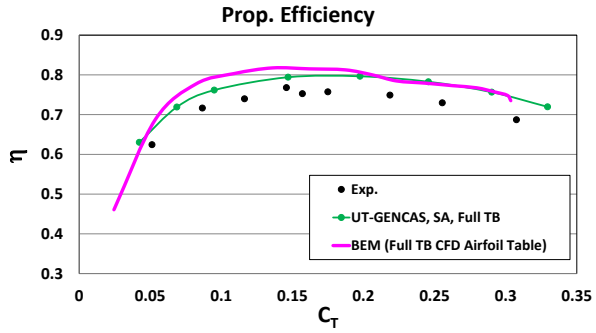


Figure 20. Propeller-B efficiency vs. Thrust

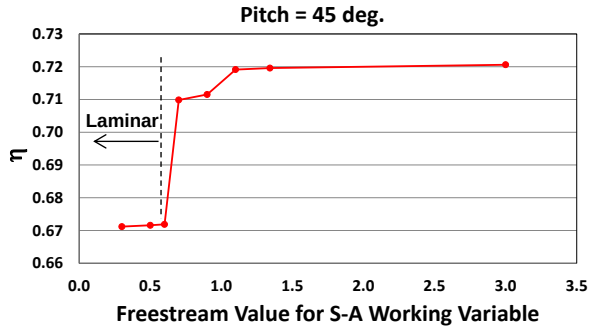


Figure 21. Efficiency vs. $\tilde{\nu}$ at $\beta = 45$ deg.

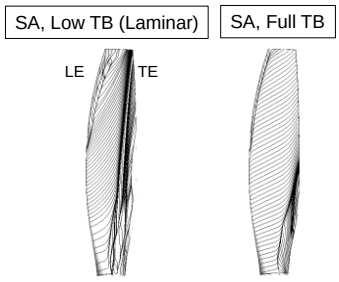


a) Suction side

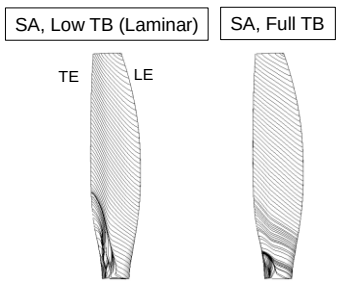


b) Pressure side

Figure 24. Surface flow pattern, $\beta = 39$ degree

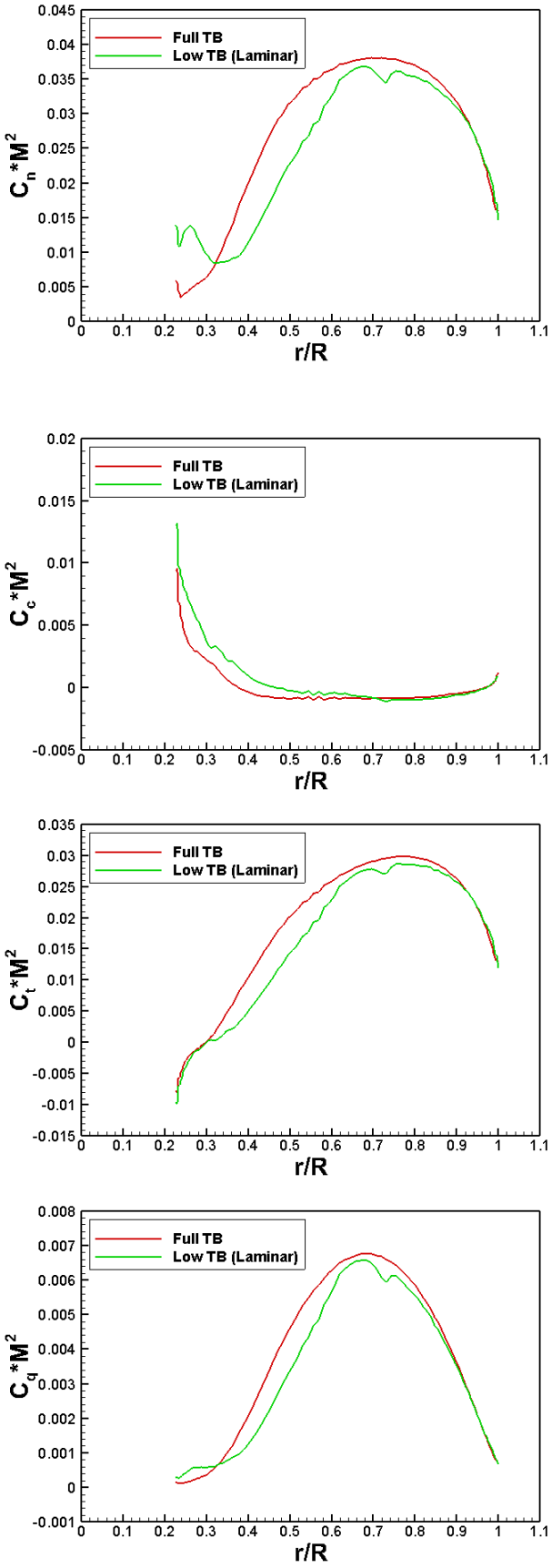


Figure 25. Blade loading, $\beta = 39$ degree

### 3.4. Propeller-C

The propeller-C is similarly sized to propeller-B with different airfoils and a slightly different pitch and twist distribution. It was also tested at UTRC's PWT with same rig used for propeller-B. Its operating condition was also maintained same as propeller-B. Figure 26 and Figure 27 compare predicted power and efficiency from UT-GENCAS with measured data. Here, simulation was carried out using low freestream $\tilde{\nu}$ value, which makes flow practically laminar. Excellent correlations with measured data were achieved for both power and efficiency, supporting the laminar flow hypothesis. As observed in propeller-B, a fully turbulent simulation resulted in over-prediction of efficiency.

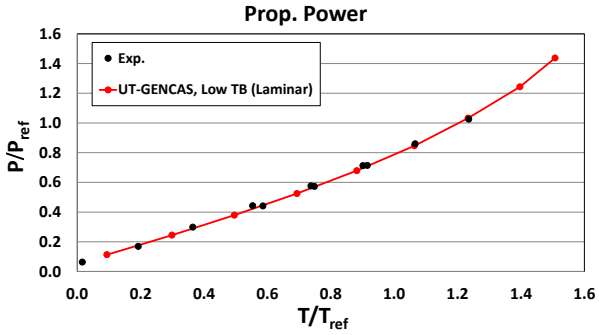


Figure 26. Propeller-C power vs. thrust

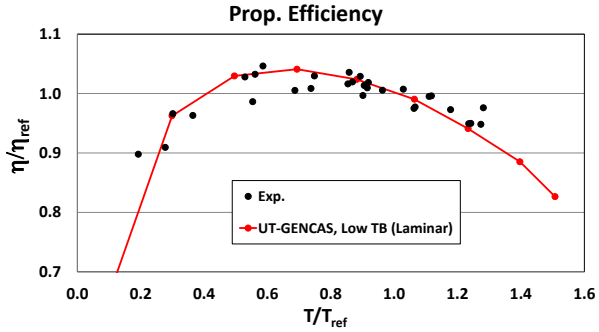


Figure 27. Propeller-C efficiency vs. thrust

## 4. CONCLUSION

A hybrid Navier-Stokes/Free-wake method has been introduced for an efficient and accurate propeller simulation. Parametric studies have been performed to establish a proper modelling approach for propeller simulation. The method has been validated for three different propellers in small scale in terms of integrated power, thrust and efficiency. Comparisons were made not only with measured data, but also with full Navier-Stokes and BEM

simulations in order to assess its accuracy with conventional methods. Overall, the correlation using hybrid method showed very good agreement with measured data, at least as good as full CFD simulation if not better. The in-house BEM code provided good correlation with fast run-time, but the solution quality relied on the accuracy of airfoil tables and a larger deviation in correlating blade angle prediction vs. CFD methods was observed. A finding from the current study indicated possible large region of laminar flow for small scale propeller tests. The Reynolds number was lower than the critical Reynolds number for small scales, and the simulation showed that the laminar flow assumption agrees well with experiment. This was confirmed from two similarly sized small scale propellers. Fully turbulent simulation over-predicted efficiency because of separation suppression and resultant higher thrust.

Advantages of hybrid method are realized by computational efficiency and the ease of simulations. Compared to full-wheel CFD simulation for 6-bladed propeller, current hybrid method was more than 4 times faster in terms of total CPU hours. Since the hybrid method uses a single blade mesh, computational time does not increase with number of blade. The blade pitch angle modification is also easy with a single blade simulation. Full-wheel simulation often requires a new mesh generation step for different pitch, unless a robust local grid deformation is employed. Another advantage of the hybrid method is that it is capable of unsteady yawed inflow simulation with a single blade grid, whereas single passage full CFD simulation is limited to 0 degree inflow.

As for future work, validation for larger scale propellers and yawed inflow conditions are recommended.

## 5. REFERENCES


1. Moffitt, B., Joo, J., Bowles, P. O., Min, B. Y., and Wake, B. E., “Subscale Modeling and Wind Tunnel Testing of Propellers,” AIAA 2013-0499, 51st AIAA Aerospace Science Meeting, Grapevine, TX, 07-10 January 2013.
2. Rajmohan, N., Sankar L. N., Bauchau, O., Makinen, S. M., Egolf, T. A., and Charles, B. D., “Application of Hybrid Methodology to Rotors in Steady and Maneuvering Flight,” American Helicopter Society 64th Annual Forum, Montreal, Canada, April 29-May 1, 2008.
3. Smith, M. J., Lim, J. W., van der Wall, B. G., Baeder, J. D., Biedron, R. T., Boyd Jr., D., Jayaraman, B., Jung, S. N., Min, B. Y., “The HART II international workshop: an assessment of the state of the art in CFD/CSD prediction,” CEAS Aeronautical Journal, Vol. 4, 2013, pp. 345-372, DOI 10.1007/s13272-013-0078-8
4. Min, B. Y. and Wake, B., “Analysis of a Hovering Rotor using UT-GENCAS: A Modified Hybrid Navier-Stokes/Free-Wake Method,” AIAA 2015-1247 , AIAA SciTech 2015, Kissimmee, FL, 5-9 January, 2015.
5. Tongchipakdee, C., “Computational Studies of the Effects of Active and Passive Circulation Enhancement Concepts on Wind Turbine Performance,” Ph. D. Dissertation, School of Aerospace Engineering, Georgia Institute of Technology, Atlanta, GA, 2007.
6. Fang, Y., and Menon, S., “A Two-Equation Subgrid Model for Large-Eddy Simulation of High Reynolds Number Flows,” AIAA 2006-116, 44th AIAA Aerospace Sciences Meeting and Exhibit, Reno, Nevada, 9-12 January, 2006.
7. Ni, R. H., "A multiple-grid scheme for solving the Euler equations," *AIAA Journal*, vol. 20, no. 11, 1982.
8. User Guide version STAR-CCM+ 10.02
9. Moffit, B. A., Bradley, T. H., Parekh, D. E., and Mavris, D., "Validation of Vortex Propeller Theory for UAV Design with Uncertainty Analysis," in 46th AIAA Aerospace Sciences Meeting and Exhibit, Reno, NV, AIAA 2008-406, January 7-10, 2008.
10. Drela, M,. *A User's Guide to MSES 3.0.* s.l. : M.I.T. Aerospace Computational Design Lab, March 2004.
11. Drela, M. *MSES: Multi-Element Airfoil Design and Analysis Software.* s.l. : M.I.T. Aerospace Computational Design Lab, 1994.